



Sharif University of Technology

Scientia Iranica

Transactions F: Nanotechnology

www.scientiairanica.com



# New molecular self-assembled monolayers on a gold electrode for simultaneous determination of epinephrine and uric acid

M. Mazloun-Ardakani\*, A. Dehghani-Firouzabadi, A. Benvidi,  
Bi-Bi F. Mirjalili and M.A. Mirhoseini

Department of Chemistry, Faculty of Science, Yazd University, Yazd, Iran.

Received 4 October 2013; received in revised form 15 July 2014; accepted 1 December 2014

## KEYWORDS

Self-assembled  
monolayer membrane;  
Quartz crystal  
microbalance;  
Epinephrine; Uric  
acid.

**Abstract.** In the present paper, we use a gold electrode modified by a 2-(3, 4-dihydroxy phenyl) benzothiazole self-assembled monolayer (DHT-SAM) for determination of epinephrine (EP) and Uric Acid (UA). Initially, DHT-SAM was characterized by different techniques. CV was used to investigate the redox properties of the modified electrode at various scan rates. The apparent charge transfer rate constant,  $k_s$  and transfer coefficient ( $\alpha$ ) were calculated. Next, electro oxidation of epinephrine (EP) and Uric Acid (UA) on a gold electrode modified by a self-assembled monolayer of DHT mediated was investigated. At the optimum pH of 7.0, the oxidation of EP occurs at a potential about 200 mV less positive than that of an unmodified gold electrode. The values of transfer coefficients ( $\alpha = 0.35$ ), catalytic rate constant ( $k = 4.4 \times 10^4 \text{ M}^{-1} \text{ s}^{-1}$ ) and diffusion coefficient ( $D = 1.03 \times 10^{-6} \text{ cm}^2 \text{ s}^{-1}$ ) were calculated for EP, using electrochemical approaches. Differential Pulse Voltammetry (DPV) exhibited a linear dynamic range over a concentration range of 0.5–400.0  $\mu\text{M}$  and a detection limit (3s) of 0.11  $\mu\text{M}$  for EP in pH = 7. Finally, simultaneous determination of EP and UA at the modified electrode was described and used for determination of EP in the EP ampoule.

© 2014 Sharif University of Technology. All rights reserved.

## 1. Introduction

Self-Assembled Monolayers (SAMs) have recently become very important due to their potential applications to biosensors, nanotechnology and bio molecular electronics. Sensitivity, selectivity, stability, the possibility of introducing different chemical functionalities, short response time and ease of preparation are all advantages of SAMs [1,2]. Different methods, such as scanning tunneling microscopy, cyclic voltammetry, square wave voltammetry, electrochemical impedance spectroscopy [3] and quartz crystal microbalance [4],

can be undertaken for characterization and study of the SAM modified surfaces.

Epinephrine (EP) or adrenaline belongs to a catecholamine group that is produced only by the adrenal glands from the amino acids, phenylalanine and tyrosine. EP is a hormone that can increase heart rate, flex blood vessels and participate in the fight/flight response of the sympathetic nervous system. Many diseases are related to changes of EP concentration in living systems [5]. EP has a significant role in nervous chemical processes. Therefore, detection and quantification of EP is useful for nerve physiology. Some methods have been reported for the determination of EP, such as chromatography [6], spectrophotometry [7] and electrochemical methods [8–14]. Electrochemical methods provide a cost effective, simple and quick

\*. Corresponding author. Fax: +98 351 8210644  
E-mail address: mazloun@yazd.ac.ir (M.  
Mazloun-Ardakani)

way of analyzing biologically and environmentally important molecules. The EP electrooxidation at bare electrodes is associated with problems of slow electron transfer rate and adsorptions of EP on the electrode surfaces leading to passivation. A promising approach to overcome difficulties is the use of chemically modified electrodes.

Uric Acid (UA) is a primary end product of the purine metabolism. UA is a major product of the catabolism of the purine nucleosides; adenosine and guanosine, which, in humans, are present in blood and urine. Detection of UA in the blood or urine is very important because it can be used as a powerful indicator for early warning signs of kidney disease. Abnormal levels of UA in blood serum and urine lead to several diseases; namely, gout, hyperuricaemia, pneumonia, kidney damage, and cardiovascular disease [15–17]. Simultaneous determination of EP and UA in a mixture is quite attractive to biological and chemical research because EP and UA are coexistent in the biological fluids of humans. The main problem in EP analysis is elimination of interference from UA, which results in peak overlapping. Therefore, it is difficult to be separately determined by the use of bare electrodes. To our knowledge, no study has been published so far reporting on the simultaneous determination of EP and UA using (DHT-SAM). Here, in continuation of our studies concerning the preparation of SAMs [18,19], we prepared DHT-SAM characterized by CV, EIS, STM and QCM. Then, we evaluated the analytical performance of the modified electrode for simultaneous determination of EP in a phosphate buffer solution in the presence of UA. This modified electrode was quite effective, not only in detecting EP and UA but also in simultaneous determination of these species in a mixture. Detection of the limit and the linear dynamic range for EP in this work is excellent, and is comparable with other work.

## 2. Experimental

### 2.1. Apparatus and chemicals

A potentiostat/galvanostat  $\mu$ Autolab Type III (Eco Chemie B. V.) equipped with GPES 4.9 software was used to perform all electrochemical experiments. A three-electrode cell was used at  $25 \pm 1^\circ\text{C}$ . An Ag/AgCl (KCl, sat.) electrode, a platinum wire and a DHT self-assembled monolayer gold disk electrode (Metrohm, 2 mm diameter) were used as reference, and auxiliary and working electrodes, respectively. pH measurements were carried out with a Metrohm model 691 pH/mV meter. QCM measurements were carried out with SRS QCM 200 made in the USA. Scanning Tunneling Microscopy (STM) measurements were carried out in air using a nano surface, easy scan, 2-controller,

from Switzerland. The STM images were recorded in a constant current tunneling mode using tunneling current of 0.2 nA, sample bias at 500 mV and a  $1000 \times 1000$  points/ $100 \times 100$  nm<sup>2</sup> resolution. All solutions were prepared with doubly distilled water. EP, UA and other reagents were analytical grade (Merck, Darmstadt, Germany). The buffer solutions were prepared from orthophosphoric acid and its salts in the pH range of 3.0–11.0.

### 2.2. General procedure for the synthesis of 2-(3, 4-dihydroxy phenyl) benzothiazole

A mixture of 2-aminothiophenol (1.2 mmol), 3, 4-dihydroxybenzaldehyde (1 mmol) and Al (HSO<sub>4</sub>)<sub>3</sub> (0.02 g) was heated at  $80^\circ\text{C}$  for 10 minutes. The progress of the reaction was monitored by TLC. After completion of the reaction, the mixture was cooled to room temperature, and dissolved in acetone; then, followed by addition of water, the solid product appeared. The product was re-crystallized in hot ethanol.

FT-IR(ATR, neat),  $\nu$ =3478 (OH), 1470, 1364, 1264, 1200, 1175, 1071, 1055, 765, 721 cm<sup>-1</sup> <sup>1</sup>HNMR (400 MHz, Acetone-d<sub>6</sub>):  $\delta$ : 6.98 (d, J=8.4 Hz, 1H), 7.38 (t, J=7.2 Hz, 1H), 7.51 (m, 2H), 7.67 (d, J=2 Hz, 1H), 7.96 (d, J=8.0 Hz, 1H), 8.02 (d, J=8.0 Hz, 1H), 8.50 (s, 1H), 8.69 (s, 1H).

## 3. Results and discussion

### 3.1. Preparation and characterization of DHT-SAM modified electrode

The bare gold electrode was polished to a mirror-like surface with 0.3 and 0.05  $\mu\text{m}$  Al<sub>2</sub>O<sub>3</sub> powders, respectively, and then ultrasonically cleaned in water/ethanol/water, each step 5 min, to remove physically adsorbed particles and washed with double-distilled water. Then, the electrode was cycled between 0.0 and 1.5 V vs. Ag/AgCl at scan rate of 100 mV s<sup>-1</sup> in 0.5 M H<sub>2</sub>SO<sub>4</sub>, until a stable CV was obtained (Figure 1, curve A). A constant roughness factor was obtained from the ratio of the real to geometric surface area of the electrode [20] and an attempt was made to maintain it constant in all experiments [21]. The CVs obtained on the bare Au electrodes showed a peak separation ( $\Delta E \approx 70$  mV) in the presence of a reversible marker [Fe(CN)<sub>6</sub>]<sup>3-/4-</sup>, which indicates that the electrochemical cell and the instrument system were properly configured and supported the cleanness of the electrode (inset of Figure 1).

Coating an electrode using DHT, and a formation of modified electrode DHT-SAM was investigated by the QCM and EIS methods (Figure 2). Formation of Au SAM was traced by the QCM method and shown in Figure 2(a). As this figure shows, when the crystal was immersed in an ethanol solution of 1 mM DHT, the frequency decreased over time (curve A), corresponding

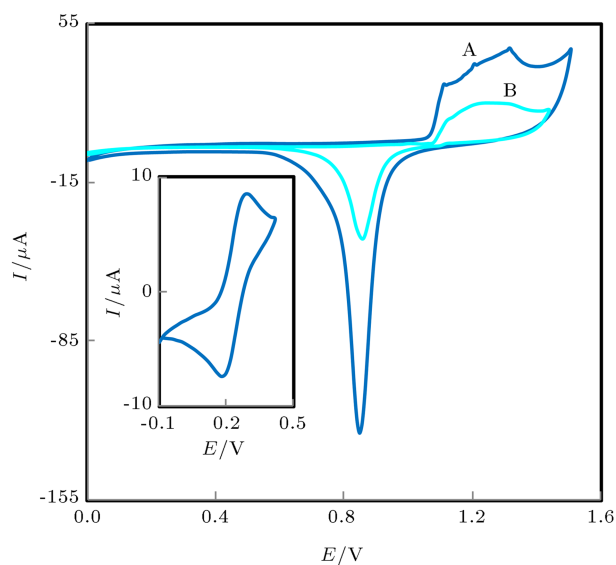


**Figure 1.** Cyclic voltammograms obtained for electrochemical oxidation/reduction of Au (A) and Au-DHT (B) in 0.5 M  $\text{H}_2\text{SO}_4$ . Inset: Cyclic voltammogram obtained in 0.1 M PBS, 0.5 mM  $[\text{Fe}(\text{CN})_6]^{3-/4-}$  for bare Au electrode. Scan rate  $100 \text{ mVs}^{-1}$  for all CVs.

to an increasing amount of DHT adsorbed on the Au electrode (curve B).

EIS also was investigated for formation of DHT-SAM on an Au electrode. The complex plane plots obtained on bare Au and Au-DHT electrodes are shown in Figure 2(b). A small semicircle (curve A) followed by a straight line in the unmodified electrode indicates the supremacy of mass diffusion limiting the effect of the electron transfer process (curve A, in the low frequency range). The respective semicircle diameter ( $R_{ct}$ ) at high frequency ranges increases by the formation of DHT-SAM on the gold electrode surface (curve B). This process has introduced a larger barrier to the interfacial charge transfer, which has been revealed by increasing the diameter of the semicircle in the spectrum. It was found that the surface has not been completely blocked, because  $R_{ct}$  is not infinite and the diffusion line (Warburg impedance) still exists.

Figure 3 shows STM images for clean Au (a) and a modified electrode (b). As this figure shows, the clean gold electrode has a flat surface, which can act as an ideal template for the SAM of our interest. From the STM image of the Au-DHT surface shown in Figure 3(b), it can be seen that this layer is formed. Since the bare Au surface has not shown such a topology, the observed image can be attributed to the presence of DHT on the surface.

### 3.2. Electrochemical behaviors of the DHT

The electrochemical behavior of the DHT was investigated by CV in aqueous solution. CVs for the modified

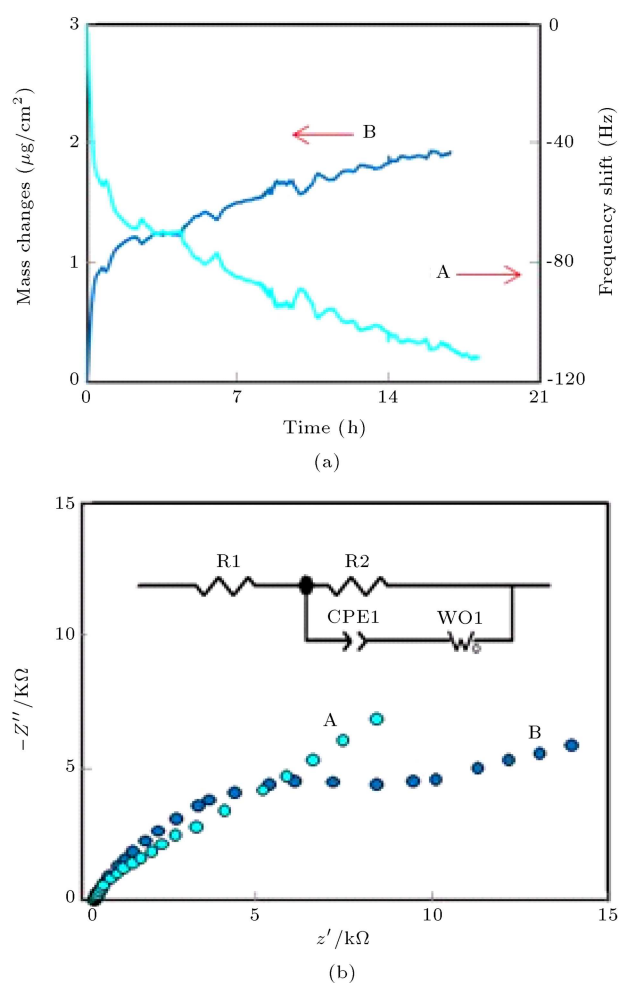


**Figure 2.** (a) Frequency shift (curve A) and the mass changes (curve B) as a function of time during formation of DHT onto Au electrode surface of the quartz crystal. (b) EIS obtained on (A) bare Au and (B) DHT-SAM electrode in 0.1 M PBS, 0.5 mM  $[\text{Fe}(\text{CN})_6]^{3-/4-}$ , ac potential 5 mV, and frequency range of 10 kHz to 0.1 Hz. Inset show equivalent circuit.

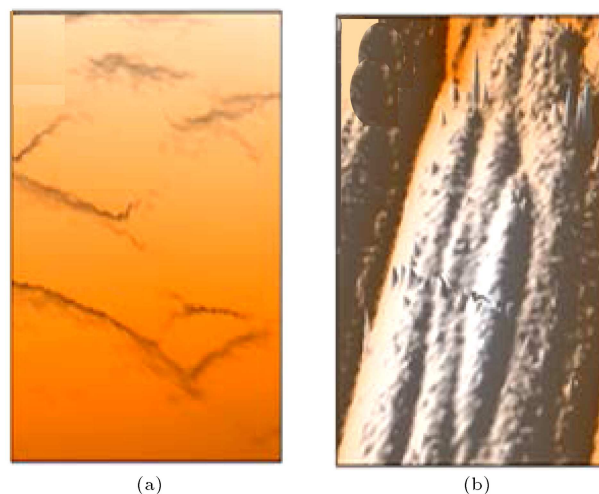


**Figure 3.** STM image obtained on (a) bare Au, and (b) DHT-SAM electrodes.

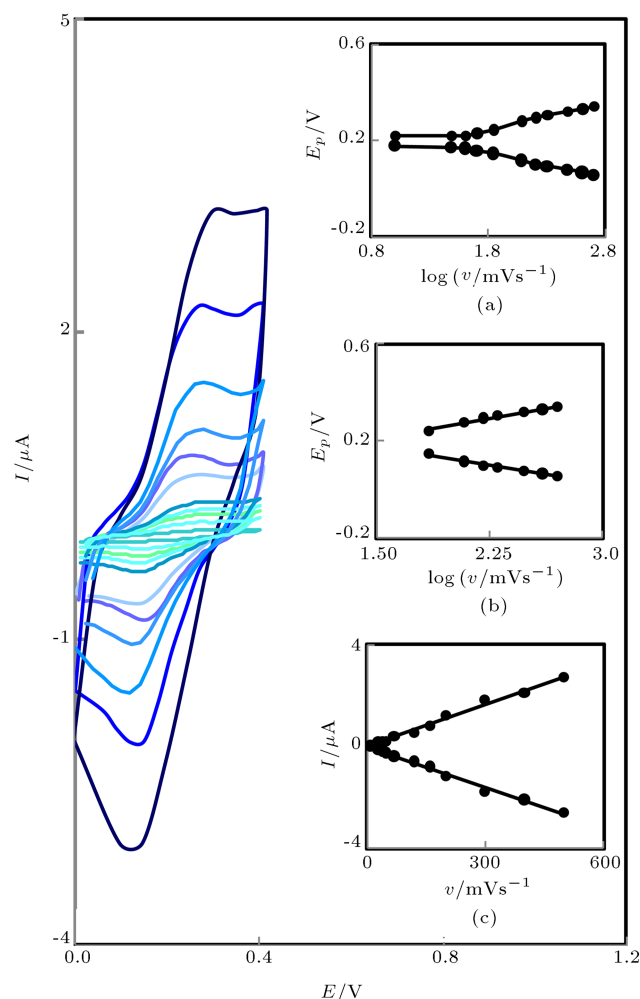


**Figure 4.** Cyclic voltammograms obtained at DHT-SAM in 0.1 M phosphate buffer (pH 7.0) at various scan rates from 10 to 500  $\text{mV s}^{-1}$ . Insets: (a) Variation of  $E$  versus the logarithm of scan rate, (b) variation of  $E$  versus the logarithm of scan rate for scan rates higher than 70  $\text{mV s}^{-1}$ , and (c) variations of  $I_{pa}$  versus scan rate.

electrode, at different scan rates (10.0–500.0  $\text{mV s}^{-1}$ ), were obtained in a 0.1 M phosphate buffer of pH = 7.0, as shown in Figure 4. As this figure shows, at scan rates of below 50  $\text{mV s}^{-1}$ , the cyclic voltammogram exhibits an anodic peak at 0.235 V in the forward potential scan, and a cathodic peak at 0.135 V in the reverse scan. Half wave potential ( $E_{1/2}$ ) and  $\Delta E$  (the difference between  $E_{pa}$  and  $E_{pc}$ ) were 0.185 V and 0.1 V vs. Ag/AgCl, respectively.  $\Delta E$  is greater than  $59/n$  mV, expected for a reversible system. Therefore, the redox couple in the modified electrode shows a quasi-reversible behavior in an aqueous medium [22]. Inset (a) of Figure 4 shows the magnitudes of peak potentials ( $E_{pa}$  and  $E_{pc}$ ) as a function of the potential scan rate. According to Laviron [23], there are general expressions for the voltammetric response of the surface-confined electroactive species at very dilute concentrations, as:

$$E_p = E^\circ + A \ln \left[ \frac{1 - \alpha}{m} \right], \quad (1)$$

$$E_{pc} = E^\circ + A \ln \left[ \frac{a}{m} \right], \quad (2)$$

For  $\Delta E_p > 200/n$  mV:

$$\log K_S = \alpha \log(1 - \alpha) + (1 - \alpha) \log \alpha - \log \left( \frac{RT}{Fnv} \right) - \frac{an_\alpha F \Delta E_p (1 - \alpha)}{2.3RT}, \quad (3)$$

where  $A = \frac{RT}{(1 - \alpha)nF}$ ,  $B = \frac{RT}{anF}$ ,  $m = \left( \frac{RT}{KF} \right) \left( \frac{K_S}{nv} \right)$  and other terms have their usual significance.

We found that the  $E_p$  values are proportional to the logarithm of the potential scan rate, for scan rates higher than 70  $\text{mV s}^{-1}$  (inset (b) of Figure 4).  $\Delta E$  increased by increasing the scan rate, due to kinetic limitation [22]. The slope of the linear segment is equal to  $2.303RT/(1 - \alpha)nF$  for the anodic peaks and  $-2.3RT/nF\alpha$  for cathodic peaks. Using such slopes, the values of the anodic and cathodic transfer coefficient for DHT-SAM in the presence of a 0.1 M phosphate buffer were calculated to be 0.42 and 0.58, respectively. Also, the value of  $k_s$  was found to be 1.5  $\text{s}^{-1}$ . The anodic and cathodic peak currents were plotted vs. scan rate, as shown in the inset (c) of Figure 4. Anodic and cathodic peak current values were linearly dependent on the different scan rates over the 10–500  $\text{mV s}^{-1}$  range, with a linear relationship between peak current and potential scan rate. The surface coverage of the electrode was made using the following equation [22]:

$$I_p = n^2 F^2 A \Gamma \frac{nv}{4RT}, \quad (4)$$

where  $n$  represents the number of electrons involved in the reaction,  $A$  is the surface area (0.0314  $\text{cm}^2$ ) of the electrode,  $\Gamma$  ( $\text{mol cm}^{-2}$ ) is the surface coverage, and other symbols have their usual meanings. From the slope of the anodic peak currents versus scan rate (Figure 4, inset (c)), the calculated surface coverage of DHT is  $4.6 \times 10^{-11}$   $\text{mol cm}^{-2}$  for  $n = 2$ .

### 3.3. Effect of pH

Since the DHT has a catechol group, we anticipated that the electrochemical response of the mediator would be pH dependent. In order to ascertain this, the voltammetric responses of DHT were carried out at pH of 3.0–11.0 with buffer solutions, and it was observed that the electrochemical response of the DHT molecule is dependent on pH. A straight line was obtained with a slope value of 0.064 mV per pH in the pH ranges of 3.0–11.0. So, there is a transfer of two electrons and two protons in the redox reaction of DHT in the pH range of 3.0–11.0. Also, the effect of pH on the response of

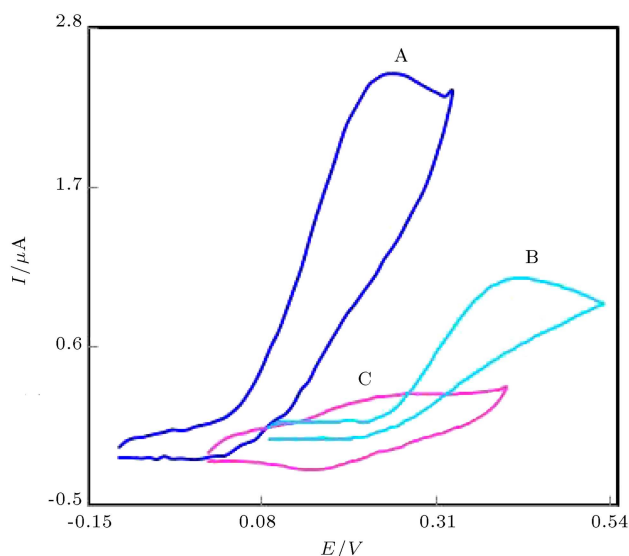


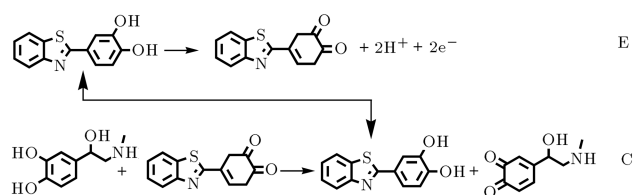
**Figure 5.** Cyclic voltammograms obtained at (A) DHT-SAM, (B) bare electrode in 0.1 M phosphate buffer solution (pH 7.0) at a scan rate of  $30 \text{ mV s}^{-1}$  containing  $80.0 \text{ } \mu\text{M}$  EP, and (C) the DHT-SAM in the phosphate buffer.

EP was investigated under different pH. By increasing the pH, the potentials of the peak shift to negative values. According to the current peak, optimum pHs were 5 to 9. Since more biological reactions occur in a neutral environment, the electrochemical behavior of the DHT-SAM was studied at pH = 7 in further work.

### 3.4. Electrocatalytic oxidation of EP at the DHT-SAM

CVs of DHT-SAM and an unmodified gold electrode in buffered aqueous solution (pH = 7.0), in the presence of  $80.0 \text{ } \mu\text{M}$  EP, were obtained (curves of A and B in Figure 5). For comparison, curve (C) shows the cyclic voltammogram of the DHT-modified electrode in the phosphate buffer only at a scan rate of  $30 \text{ mV s}^{-1}$ . CVs in Figure 5 indicate that the electrooxidation of EP can be catalyzed by a redox couple of DHT as mediator. Comparison of curves A and B in Figure 5 indicates the anodic peak current of the modified electrode was greatly increased in the presence of EP. Also, results at the optimum pH of 7.0 indicate that the oxidation of EP occurs at a potential about 200 mV less positive than that of an unmodified gold electrode. Based on these results, we propose an EC' catalytic mechanism, shown in Scheme 1, to describe the electrochemical oxidation of EP at DHT-SMA electrodes. In this scheme, EP is oxidized in the catalytic (C) reaction by the oxidized form of DHT produced at the electrode surface via an electrochemical (E) reaction.

The effect of scan rate on the electrocatalytic oxidation of EP at the DHT-SAM was investigated by cyclic voltammetry. As Figure 6 shows, the oxidation peak potential shifts with increasing scan



**Scheme 1.** Mechanism of electrocatalytic reaction between EP and DHT.

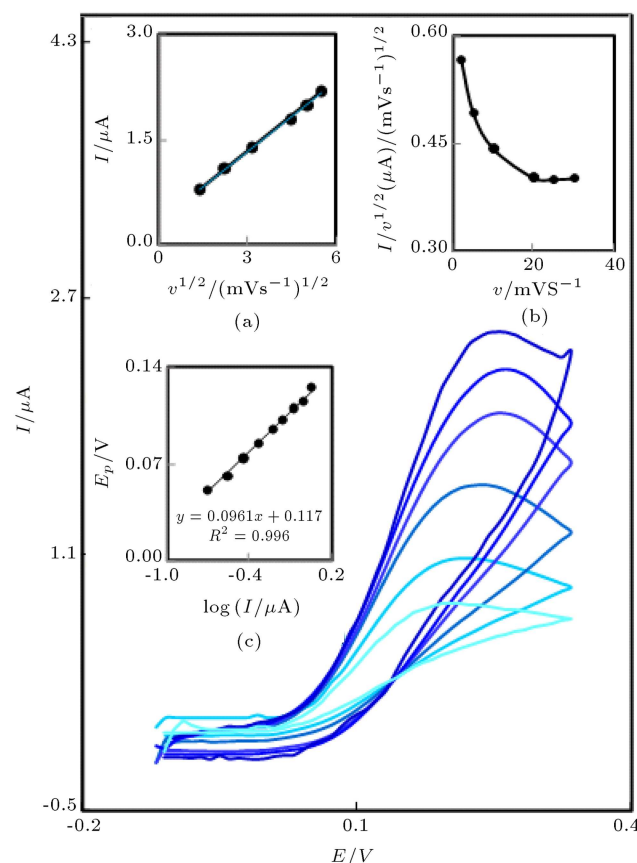


**Figure 6.** CVs of DHT-SAM in 0.1 M PBS (pH 7.0) containing  $80 \text{ } \mu\text{M}$  EP at various scan rates, from inner to outer scan rates of 2, 5, 10, 20, 25 and  $30 \text{ mV s}^{-1}$ , respectively. Insets: Variation of (a) anodic peak current vs.  $\nu$ , (b) normalized current  $I_p/\nu^{1/2}$  vs.  $\nu$ , and (c) the Tafel plot derived from the cyclic voltammogram.

rates towards a more positive potential, confirming the kinetic limitation of the electrochemical reaction. Also, a plot of peak height ( $I_p$ ) against the square root of scan rate ( $\nu^{1/2}$ ) was constructed (Figure 6, inset (a)), which was found to be linear, suggesting that at sufficient overpotential, the process is diffusion-controlled. Inset (b) of Figure 6 shows the variation of the scan rate normalized current ( $I_p/\nu^{1/2}$ ), with the scan rate expected for an electrocatalytic EC' reaction. Inset (c) of Figure 6 shows a Tafel plot that was drawn from points shown in the cyclic voltammogram. A transfer coefficient of  $\alpha = 0.38$  can be estimated from the slope of the Tafel plot that was 0.0961.

### 3.5. Chronoamperometric measurements

The chronoamperometric behavior of DHT-SAM was examined in the absence, and in the presence, of EP. Chronoamperometric measurements of different concentrations of EP solution were done by setting the working electrode potential at 250 mV, and different concentrations of EP are depicted in Figure 7. The current for the electrochemical reaction is described by the Cottrell equation [22]:

$$I = nFAD^{\frac{1}{2}}C_b\pi^{-\frac{1}{2}}t^{-\frac{1}{2}}, \quad (5)$$

where  $D$  and  $C_b$  are the diffusion coefficient ( $\text{cm}^2 \text{s}^{-1}$ ) and the bulk concentration ( $\text{mol cm}^{-3}$ ) of EP, respectively. Inset (a) in Figure 7 shows the experimental plots of  $I$  versus  $t^{-1/2}$  for different concentrations of EP. Inset (b) in Figure 7 shows the slopes of the resulting straight lines plotted versus EP concentration. Using the slope of the linear relation in Figure 7(b), and based on the Cottrell equation, we estimate the diffusion coefficient of EP to be  $1 \times 10^{-6} \text{ cm}^2 \text{s}^{-1}$ . We have also used the chronoamperometric method of Galus to

evaluate the catalytic rate constant,  $k/\text{M}^{-1}\text{S}^{-1}$ , for the reaction between EP and the DHT [24]:

$$\frac{I_{\text{cat}}}{I_L} = \gamma^{\frac{1}{2}} \left[ \pi^{\frac{1}{2}} \text{erf}(\gamma^{\frac{1}{2}}) + \exp\left(\frac{-\gamma}{\gamma^{\frac{1}{2}}}\right) \right], \quad (6)$$

where  $I_L$  is the limited current in the absence of EP,  $I_C$  is the catalytic current of EP at the DHT, and  $\gamma = kC_b t$  ( $C_b$  is the bulk concentration of EP) is the argument of the error function. In the cases where  $\gamma$  exceeds 2, the error function is almost equal to 1 and the above equation can be reduced to:

$$\frac{I_{\text{cat}}}{I_L} = \pi^{\frac{1}{2}} \gamma^{\frac{1}{2}} = \pi^{\frac{1}{2}} (kC_b t)^{\frac{1}{2}}, \quad (7)$$

where  $t$  is the time elapsed.  $k$  can be obtained for a given EP concentration based on the slope of the  $I_C/I_L$  vs.  $t^{1/2}$  plot that is shown in inset (c) of Figure 7. The average value of  $k$  was found to be  $k = 4.4 \times 10^4 \text{ M}^{-1}\text{s}^{-1}$ . The value of  $k$  also explains the sharp feature of the catalytic peak observed for the catalytic oxidation of EP at the surface of the DHT-SAM.

### 3.6. Calibration plot and detection limit

Detection limit can be calculated by differential pulse voltammetry because DPV is a powerful electrochemical technique that can be applied in both electro kinetic and analytical measurements. The responses were linear, with EP concentrations ranging from 0.5–400.0  $\mu\text{M}$ . From the analysis of data, we estimated that the lower limit of the detection of EP is approximately 0.11  $\mu\text{M}$ , based on the following equation:

$$\text{DL} = 3s_b/m,$$

where  $s_b$  is the relative standard deviation of the blank for 10 measurements by DPV, and  $m$  is the slope of the calibration plot.

### 3.7. Simultaneous determination of EP and UA

Since the voltammetric signals of EP and UA are close to each other in 0.350 and 0.444 V at the gold electrode, respectively [25,26], the use of chemically-modified electrodes greatly increases the selectivity and sensitivity toward these analytes. DPV was used for the determination of EP and UA at the DHT-SAM because of its higher current sensitivity and better resolution than cyclic voltammetry. The obtained results show two well-distinguished anodic peaks at potentials of 172 and 410 mV, indicating that the simultaneous determination of EP and UA is possible at the DHT-SAM (Figure 8). The sensitivities of the modified electrode towards EP in the absence and presence of UA ( $0.0063 \mu\text{A } \mu\text{M}^{-1}$  and  $0.0066 \mu\text{A } \mu\text{M}^{-1}$ ) are very close to each other. Therefore, simultaneous or independent measurements of the two analytes are feasible without any interference, which indicate that

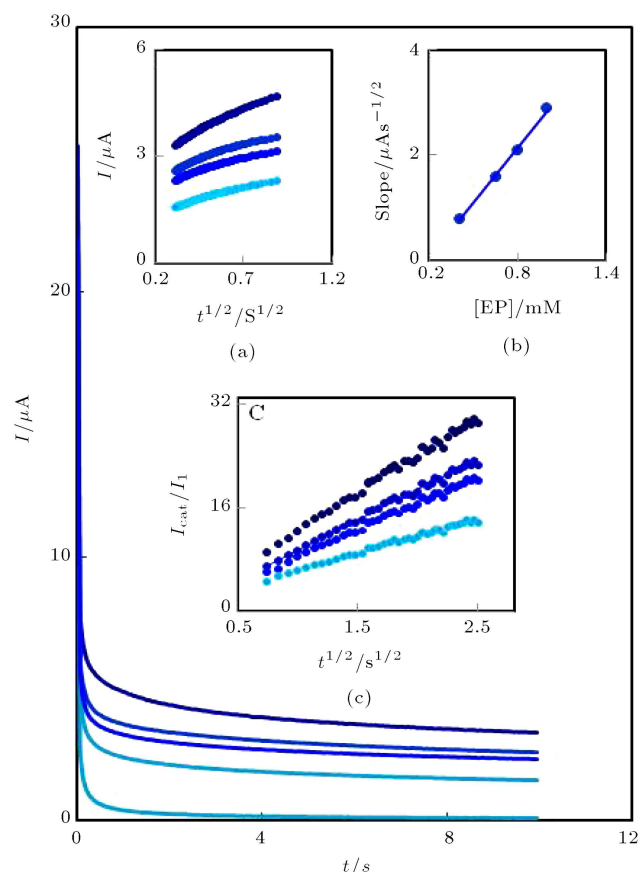


**Figure 7.** Chronoamperograms obtained at DHT-SAM in 0.1 M phosphate buffer solution (pH 7.0) for EP concentrations of 0.0, 0.4, 0.65, 0.8 and 1.0 mM. Insets: (a) Plots of  $I$  vs.  $t^{-1/2}$  obtained from the chronoamperogram data; (b) plot of the slope of the straight lines against the EP concentration; and (c) dependence of  $I_C/I_L$  derived from the data of chronoamperograms.

the oxidation processes of EP and UA at the DHT-SAM are independent.

### 3.8. Determination of EP and UA in a real sample

One mL of an EP ampoule was diluted to 10 mL with the phosphate buffer solution (0.1 M, pH 7.0).

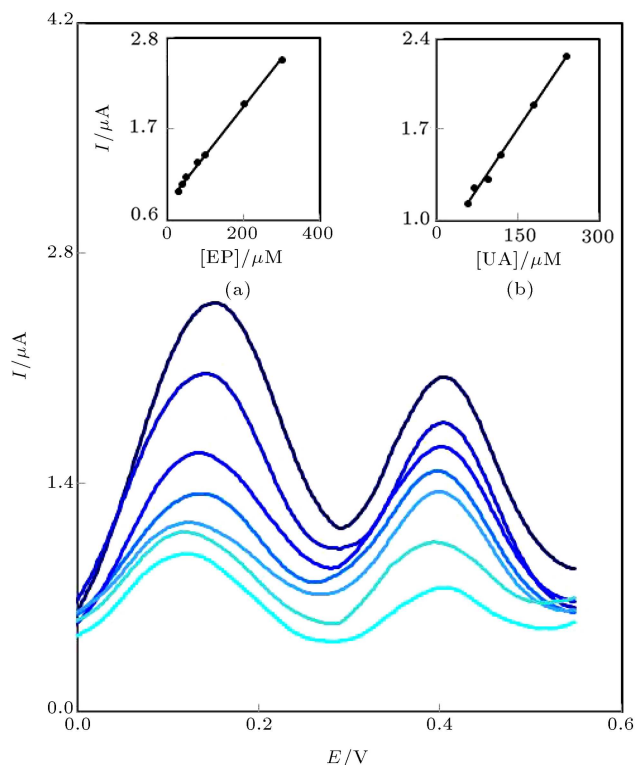


**Figure 8.** Differential pulse voltammograms obtained DHT-SAM in 0.1 M phosphate buffer solution (pH 7.0) containing different concentrations of EP and UA (from inner to outer) mixed solutions of 30.0+50.0, 40.0+60.0, 50.0+80.0, 80.0+100.0, 100.0+150.0 and 300.0+250.0  $\mu\text{M}$  respectively. Insets: (a) Plot of the peak currents as a function of EP concentration; and (b) plot of the peak currents as a function of UA concentrations. Scan rate: 25  $\text{mV s}^{-1}$ ; modulation time: 0.05 s; and pulse amplitude: 0.02 V.

Then, different volumes of the diluted solution were transferred into each of a series of 10 mL volumetric flasks and diluted to the mark with phosphate buffer. A 10 mL aliquot of this test solution was placed in the electrochemical cell. The capability of this modified electrode for catalytic oxidation of EP in ampoule was investigated without interference from recipients and other drugs encountered by DPV. Therefore, we studied the electrochemical behavior of DHT-SAM in 0.1 M phosphate buffer (pH 7.0) containing each pharmaceutical preparation. The determination of EP in pharmaceutical samples was carried out by the standard addition method to prevent any matrix effect. The  $I_p$  was measured at the oxidation potential of EP. This procedure was repeated five times, and the average amount of EP in the ampoule was found to be 0.97 mg; a value well in agreement with the nominal value of the ampoule label (1.0 mg). Also, a synthetic solution was prepared by adding 1 mL of standard EP and UA solutions into a series of 10 mL volumetric flasks and diluting to volume with the diluted ampoule sample. The DPVs were recorded and the anodic peak currents were measured at the oxidation potentials of EP and UA; the results are given in Table 1. In order to evaluate the analytical applicability of the proposed method, it was also applied to the determination of EP in urine and human blood serum samples. Therefore, different amounts of EP were spiked to the sample and analyzed by the proposed method. The results for determination of EP in real samples are given in Table 2. Satisfactory recovery of the experimental results was found for EP.

### 3.9. Repeatability, reproducibility and stability of DHT-SAM

DPV was used for the electrode capability in generation of a repeatable response at pH 7.0 for five measurements. The RSD was calculated as 1.3 and 1.9% for 50 and 80  $\mu\text{M}$  of EP, respectively, which indicates that the repeatability of DHT-SAM is satisfactory. In addition, the stability of the DHT-SAM was tested. A well-

**Table 1.** Determination of EP and UA in synthetic solutions.

Sample	Spiked ( $\mu\text{M}$ )		Found ( $\mu\text{M}$ ) <sup>a</sup>		Recovery (%)	
	EP	UA	EP	UA	EP	UA
1	0.0	0.0	20.0	—	—	—
2	100.0	0.0	121.1	—	101.1 $\pm$ 1.6	—
3	150.0	0.0	160.8	—	99.8 $\pm$ 2.5	—
4	200.0	0.0	219.2	—	99.6 $\pm$ 1.6	—
5	5.0	50.0	25.2	49.8	101.3 $\pm$ 2.4	99.6 $\pm$ 3.5
6	10.0	100.0	29.2	99.8	97.3 $\pm$ 3.6	99.8 $\pm$ 2.4
7	20.0	150.0	40.3	151.0	100.7 $\pm$ 2.3	99.2 $\pm$ 1.7
8	50.0	100.0	71.5	100.8	103.0 $\pm$ 1.4	100.8 $\pm$ 3.2
9	100.0	150.0	119.8	151.1	99.8 $\pm$ 2.5	100.7 $\pm$ 4.1

<sup>a</sup>: Mean value for five replicate measurements.



**Table 2.** Determination of EP in urine and human blood serum using DHT-SAM by standard addition method.

Sample	Added ( $\mu\text{M}$ )	Found ( $\mu\text{M}$ ) <sup>a</sup>	Recovery (%)
Urine	10.0	10.1	101.0 $\pm$ 1.1
	20.0	19.8	99.0 $\pm$ 3.4
	30.0	29.3	97.6 $\pm$ 2.5
Human	10.0	9.8	98.0 $\pm$ 2.5
Blood	20.0	20.3	101.5 $\pm$ 1.5
Serum	30.0	30.1	100.3 $\pm$ 3.5

<sup>a</sup>: Mean value for five replicate measurements.

defined wave of EP can be obtained after DHT-SAM at the Au electrode for 24 h in the 1.0 mM DHT at the ambient temperature, and the peak current remains the same after placing the electrode in the phosphate buffer solution for 3 h. The peak current values were detected with a relative standard deviation R.S.D of 1.9% ( $n = 5$ ). The result indicates that the electrodes have a high stability.

### 3.10. Interference study

On the determination of 50.0  $\mu\text{M}$  EP, the influence of some common interference was investigated. The tolerance limit was taken as the maximum concentration of foreign substances, which caused an approximately  $\pm 5\%$  relative error in the determination. The results showed that 10 fold of  $\text{Na}^+$ ,  $\text{K}^+$ ,  $\text{SO}_4^{2-}$ ,  $\text{NO}_3^-$ , glucose, sucrose, fructose, glutamic acid, N-acetyl-L-cysteine, leucine, glycine, acetaminophen, uric acid, folic acid and tryptophan did not affect the determination of EP. But ascorbic acid showed interference on determination of EP. For solving the interference

of these species, we can adjust the pH solution to 7.0. In this pH, ascorbic acid exists as anions form. By coating the modified electrode surface with 10  $\mu\text{L}$  of 5.0% (v/v) Nafion solution diluted with ethanol, the surface of the electrode is in negative charge, which repels the anionic form of ascorbic acid, while showing enhanced interaction with epinephrine. So, oxidation peaks for ascorbic acid shift to positive potentials.

## 4. Conclusion

In this work, we have prepared and characterized a DHT self-assembled monolayer at a gold surface by EIS, QCM, STM and CV methods for the first time, and then the DHT self-assembled Au electrode has been used for simultaneous determination of EP and UA. High sensitivity, low detection limit, ease of preparation, and high repeatability and stability of the modified electrode are the advantages of the proposed electrode. The modified electrode displays higher selectivity in voltammetric measurements of EP and UA in their mixture solution. Table 3 shows some analytical parameters, such as detection limit and linear range for electroanalysis of EP by the proposed electrode in comparison with some other electrochemical procedure. Compared with other sensors reported previously [10,11,19,27-29], our proposed sensor exhibited a satisfactory detection limit and linear range.

## Acknowledgments

The authors wish to thank the Yazd University Research Council, IUT Research Council, and Excellence in Sensors for financial support of this research.

**Table 3.** Comparison of some electrochemical procedures used in the determination of EP.

Electrode	Modifier	Method	pH	Linear range ( $\mu\text{M}$ )	Detection limit ( $\mu\text{M}$ )	Ref.
Carbon paste	MCM/ZrO <sub>2</sub> nanoparticles	Voltammetry	6	1.0-2500.0	0.5	10
Carbon paste	2,2'-[1,2 ethanediylbis (nitrilomethylidene)]-bishydroquinone	Voltammetry	7	5.0-600	1.0	11
Gold	2-(2,3-dihydroxy phenyl)-1,3-dithiane	Voltammetry	8	0.7-500.0	0.51	19
Gold electrode	Gold nanoparticles	Voltammetry	7	0.1-200.0	0.06	27
Gold electrode	Homocysteine	Voltammetry	4.1	50.0-800.0	0.1	28
Glassy carbon	Poly(cafeic acid)	Voltammetry	—	2.0-80.0	0.2	29
Gold	2-(3,4-dihydroxy phenyl) benzothiazole	Voltammetry	7.0	0.5-400.0	0.11	This work



## References

1. Zhang, S., Peng, T. and Yang, C.F. "A piezoelectric gene-sensor using actinomycin D-functionalized nanomicrospheres as amplifying probes", *J. Electroanal. Chem.*, **522**(2), pp. 152-157 (2002).
2. Nagaraju, D.H., Pandey, R.K. and Lakshminarayanan, V. "Electrocatalytic studies of cytochrome c functionalized single walled carbon nanotubes on self-assembled monolayer of 4-ATP on gold", *J. Electroanal. Chem.*, **627**(1), pp. 63-68 (2009).
3. Karimi Shervedani, R., Akrami, Z. and Sabzyan, H. "Nanostructure molecular assemblies constructed based on ex-situ and in-situ layer-by-layer ferrioximation characterized by electrochemical and scanning tunneling microscopy methods", *J. Phys. Chem. C*, **115**(16), pp. 8042-8055 (2011).
4. Su, X.L and Li, Y. "A self-assembled monolayer-based piezoelectric immunosensor for rapid detection of Escherichia coli O157: H7", *Biosens. Bioelectron.*, **19**(6), pp. 563-574 (2004).
5. Banks, W.A. "Enhanced leptin transport across the blood-brain barrier by  $\alpha$ 1-adrenergic agents", *Brain Res.*, **899**(1), pp. 209-217 (2001).
6. Shelkownikov, S. and Gonick, H.C. "Peroxyinitrite but not nitric oxide donors destroys epinephrine: HPLC measurement and rat aorta contractility", *Life Sci.*, **75**(23), pp. 2765-2773 (2004).
7. Solich, P., Polydorou, C.K., Koupparis, M.A. and Efsthathiou, C.E. "Automated flow-injection spectrophotometric determination of catecholamines (epinephrine and isoproterenol) in pharmaceutical formulations based on ferrous complex formation", *J. Pharm. Biomed. Anal.*, **22**(5), pp. 781-789 (2000).
8. Ozoemena, K.I. and Nkosi, D.J. "Pillay, influence of solution pH on the electron transport of the self-assembled nanoarrays of single-walled carbon nanotube-cobalt tetra-aminophthalocyanine on gold electrodes: Electrocatalytic detection of epinephrine", *Electrochim. Acta*, **53**(6), pp. 2844-2851 (2008).
9. Li, Y., Umasankar, Y. and Chen, S.M. "Multiwalled carbon nanotubes with poly (NDGACHi) biocomposite film for the electrocatalysis of epinephrine and norepinephrine", *Anal. Biochem.*, **388**(2), pp. 288-295 (2009).
10. Mazloun-Ardakani, M., Dehghani-Firouzabadi, A., Rajabzade, N., Sheikh-Mohseni, M.A., Benvidi, A. and Abdollahi-Alibeik, M. "MCM/ZrO<sub>2</sub> nanoparticles modified electrode for simultaneous and selective voltammetric determination of epinephrine and acetaminophen", *J. Iran. Chem. Soc.*, **9**, pp. 1-5 (2012).
11. Mazloun-Ardakani, M., Rajabzade, N., Dehghani-Firouzabadi, A., Sheikh-Mohseni, M.A., Benvidi, A., Naeimi, H., Akbari, M. and Karshenas, A. "Carbon nanoparticles and a new derivative of hydroquinone for modification of a carbon paste electrode for simultaneous determination of epinephrine and acetaminophen", *Anal. Methods*, **4**, pp. 2127-2133 (2012).
12. Beitollahi, H., Mazloun-Ardakani, M., Ganjipour, B. and Naeimi, H. "Novel 2,2'-[1,2-ethanediylbis (nitriloethylidyne)]-bis-hydroquinone double-wall carbon nanotube paste electrode for simultaneous determination of epinephrine, uric acid and folic acid", *Biosens. Bioelectron.*, **24**(3), pp. 362-368 (2008).
13. Mazloun-Ardakani, M., Beitollahi, H., Sheikh Mohseni, M.A., Benvidi, A., Naeimi, H., Nejati-Barzoki, M. and Taghavinia, N. "Simultaneous determination of epinephrine and acetaminophen concentrations using a novel carbon paste electrode prepared with 2,2'-[1,2 butanediylbis (nitriloethylidyne)]-bis-hydroquinone and TiO<sub>2</sub> nanoparticles", *Colloids Surf. B*, **76**(1), pp. 82-87 (2010).
14. Wang, H.S., Huang, D.Q. and Liu, R.M. "Study on the electrochemical behavior of epinephrine at a poly(3-methylthiophene)-modified glassy carbon electrode", *J. Electroanal. Chem.*, **570**(2), pp. 83-90 (2004).
15. Pachla, L.A., Reynolds, D.L., Wright, D.S. and Kissinger, P.T. "Analytical methods for measuring uric acid in biological samples and food products", *J. Assoc. Off. Anal. Chem.*, **70**(3), pp. 1-14 (1987).
16. Shi, K. and Shiu, K.K. "Determination of uric acid at electrochemically activated glassy carbon electrode", *Electroanalysis*, **13**(16), pp. 1319-1325 (2001).
17. Mazzali, M., Kim, Y.G., Hughes, J., Lan, H.Y., Kivlighn, S. and Johnson, R.J. "An elevated serum uric acid causes kidney damage: Evidence for a novel crystal independent mechanism", *Am. J. Hypertens.*, **13**(6), pp. S36-S37 (2000).
18. Mazloun-Ardakani, M., Beitollahi, H., Amini, F., Mirkhalaf, M.K., Mirjalili, B.B.F. and Akbari, A. "Application of 2-(3,4-dihydroxyphenyl)-1,3-dithialone self-assembled monolayer on gold electrode as a nanosensor for electrocatalytic determination of dopamine and uric acid", *Analyst.*, **136**(9), pp. 1965-1970 (2011).
19. Mazloun-Ardakani, M., Beitollahi, H., Amini, M.K., Mirjalili, B.B.F. and Mirkhalaf, F. "Simultaneous determination of epinephrine and uric acid at a gold electrode modified by a 2-(2,3-dihydroxy phenyl)-1,3-dithiane self-assembled monolayer", *J. Electroanal. Chem.*, **651**(2), pp. 243-249 (2011).
20. Oesch, U.J. "Janata, electrochemical study of gold electrodes with anodic oxide films-I. Formation and reduction behavior of anodic oxides on gold", *Electrochim. Acta.*, **28**(9), pp. 1237-1246 (1983).
21. Creager, S.E., Hockett, L.A. and Rowe, G.K. "Consequences of microscopic surface roughness for molecular self-assembly", *Langmuir*, **8**(3), pp. 854-861 (1992).
22. Bard, A.J. and Faulkner, L.R., *Electrochemical Methods: Fundamentals and Applications*, Second Ed., Wiley, New York (2001).

23. Laviron, E. "General expression of the linear potential sweep voltammogram in the case of diffusionless electrochemical systems", *J. Electroanal. Chem.*, **101**(1), pp. 19-28 (1979).
24. Galus, Z. "Fundamentals of electrochemical analysis", *Ellis Horwood*, New York (1976).
25. Behera, S. and Retna Raj, C. "Self-assembled monolayers of thio-substituted nucleobases on gold electrode for the electroanalysis of NADH, ethanol and uric acid", *Sensors and Actuat. B*, **128**(1), pp. 31-38 (2007).
26. Sivanesan, A. and John, S.A. "Selective electrochemical epinephrine sensor using self-assembled monomolecular film of 1,8,15,22- tetraaminophthalocyanatonickel (II) on gold electrode", *Electroanalysis*, **20**(21), pp. 2340-2346 (2008).
27. Wang, L., Bai, J., Huang, P., Wang, H., Zhang, L. and Zhao, Y. "Self-assembly of gold nanoparticles for the voltammetric sensing of epinephrine", *Electrochem. Commun.*, **8**(6), pp. 1035-1040 (2006).
28. Zhang, H.M., Zhou, X.L., Hui, R.T., Li, N.Q. and Liu, D.P. "Studies of the electrochemical behavior of epinephrine at a homocysteine self-assembled electrode", *Talanta*, **56**(6), pp. 1081-1088 (2002).
29. Ren, W., Qun, L.H. and Li, N.B. "Simultaneous voltammetric measurement of ascorbic acid, epinephrine and uric acid at a glassy carbon electrode modified with caffeic acid", *Biosens. Bioelectron.*, **21**(7), pp. 1086-1092 (2006).

## Biographies

**Mohammad Mazloum-Ardakani** received a BS degree in Chemistry from Kashan University, Iran, in 1986, an MS degree in Analytical Chemistry from Teacher Training University, Tehran, Iran, in 1990, and a PhD degree in Analytical Chemistry from Isfahan

University, Iran, in 2000. He is currently Professor of Analytical Chemistry in the Chemistry Department of Yazd University, Iran. His main areas of interest are electroanalytical chemistry and nanoelectrochemistry.

**Afsaneh Dehghani Firuozabadi** received a BS degree in Chemistry from Yazd University, Iran, in 1998, and an MS degree in Analytical Chemistry in 2002, from Yazd University, Iran, where she is presently a PhD student in the same subject. Her main areas of interests are different electrochemical sensors.

**Ali Benvidi** received a BS degree in Chemistry from Kashan University, Iran, in 1991, an MS degree in Analytical Chemistry from Teacher Tehran University, Tehran, Iran, in 1993, and a PhD degree in Analytical Chemistry from Isfahan University of Technology, Iran, in 2005. He is currently Professor of Analytical Chemistry in the Chemistry Department of Yazd University, Iran. His main areas of interest are electroanalytical chemistry and chemometrics.

**Bi-Bi Fatemeh Mirjalili** received a BS degree in Chemistry from Alzahra University, Iran, in 1986, an MS degree in Organic Chemistry from Teacher Training University, Tehran, Iran, in 1990, and a PhD degree in Organic Chemistry from Sharif University of Technology, Tehran, Iran, in 2000. He is currently Professor of Organic Chemistry in the Chemistry Department of Yazd University, Iran. His main areas of interest are microwave assisted organic synthesis.

**Mohammad Ali Mirhoseini** received a BS degree in Chemistry from Tehran University, Iran, in 1998, an MS degree in Organic Chemistry from Amirkabir University, Iran, in 2002, and a PhD degree in Organic Chemistry from Yazd University, Iran, in 2013. His main areas of interest are microwave assisted organic synthesis.